

Synthesis and Characterization of Nanogels Incorporating *Tectona grandis* Seed Extract for Enhanced Drug Delivery

NAYKAR SHARMILA SHASHIKANT*^{ORCID} and RAMDAS T. DOLAS^{ORCID}

School of Pharmaceutical Sciences, Department of Pharmaceutics, Sandip University, Nashik-422001, India

*Corresponding author: E-mail: sharmilawagh41@gmail.com

Received: 19 December 2024;

Accepted: 30 January 2025;

Published online: 28 February 2025;

AJC-21912

This research emphasizes the formulation and analysis of nanoparticles incorporated into a nanogel utilizing *Tectona grandis* seed extract. Silver nanoparticles (AgNPs) were synthesized using silver nitrate solution, serving as silver precursor. The resulting nanoparticles were characterized through various techniques, including particle size analysis, zeta potential measurement, energy-dispersive X-ray analysis (EDX), UV-visible spectroscopy, field emission scanning electron microscopy (FESEM), Fourier-transform infrared (FTIR) spectroscopy and transmission electron microscopy (TEM). To develop the nanogel, the synthesized nanoparticles were combined with a gelling agent. The nanogel was further evaluated for parameters such as physical appearance, pH, spreadability, washability, viscosity and antibacterial activity. Among the formulations tested, batch F1 showed the highest efficacy and stability. The antimicrobial potential of the AgNPs was confirmed through the agar well diffusion method, which exhibited a 48 mm zone of inhibition against *Escherichia coli*. Additionally, a zone of inhibition was detected within 1 day on petri plates treated with 50 as well as 100 μg of silver nanoparticles. The nanogel was further evaluated for its wound healing activity using an excision wound model. Results demonstrated a significant reduction in wound area and improved healing rates in comparison to the control group, with batch F1 exhibiting the fastest wound closure within a specified period. The heightened wound healing potential arises from the combined belongings of the antibacterial property and therapeutic benefits of silver nanoparticles with *Tectona grandis* seed extract. These findings highlight the potent antibacterial and wound healing properties of *Tectona grandis* seed extract-loaded nanoparticles, indicating their potential as effective candidates for topical therapeutic applications.

Keywords: *Tectona grandis* seed extract, Silver nanoparticles, Nanogel, Antibacterial activity, *Escherichia coli*.

INTRODUCTION

In recent years, composites of multi-responsive microgels and silver nanoparticles have garnered significant attention due to their multifunctionality and potential in biomedical applications. Nanogels, which are nanoparticles composed of hydrophilic polymer networks ranging from 100-200 nm, have emerged as a versatile drug delivery system capable of encapsulating guest molecules. These systems exhibit exceptional properties, including swelling, degradation, high drug-loading capacity, enhanced stability, sustained and targeted drug release and a large surface area. These features make nanogels more efficient and productive than conventional and micro-sized delivery systems [1].

Silver nanoparticles (AgNPs) based hybrid microgels, in particular, have shown great promise as antibacterial agents and drug carriers, with potential applications in cancer and

tumor treatments [2]. However, formulating novel products, especially for topical drug delivery, remains challenging due to the need for precise composition optimization. Topical delivery methods are traditionally favoured for targeting specific skin areas, yet they demand meticulous component selection to ensure efficacy, safety and patient compliance [3,4].

Hydrogel nanoparticles, composed of crosslinked polymeric networks, are emerging as promising drug delivery platforms. These systems offer advantages in terms of controlled drug release, enhanced stability and targeted delivery, positioning them as key innovations for future therapeutic applications. Its advantages include increased drug loading efficiency, adjustable dimensions, effortless formulation, minimal adverse effects and permanency in serum. It exhibit significant capability in chemotherapy, diagnostics, tissue aiming, as well as the transfer of bioactive materials. The concept of nanoparticle-composed gels, introduced by Kabanov & Vinogradov [5], describes

bifunctional frameworks involving non-ionic polymers and polyions for polynucleotide transport [6].

Nanoscale drug delivery systems for herbal medications show great potential due to their high encapsulation efficiency, uniformity, low toxicity and enhanced stability, making them a promising future direction for herbal therapy [7]. Natural compounds, like those obtained from *Tectona grandis* (teak), hold great potential for the growth of novel medicines. The seeds of *T. grandis*, a plant from the Verbenaceae family, have been used in traditional medicine for over 2,000 years due to their various beneficial properties [8]. In this study, *T. grandis* seed extract was employed in the environmental friendly synthesis of AgNPs, serving a dual role as a reductant to convert silver ions into silver nanoparticles and as a stabilizer to prevent the aggregation of nanoparticles. This approach eliminates the need for toxic chemicals while simultaneously improving the sustainability of the nanoparticle manufacturing process, aligning with the growing interest in eco-friendly nanotechnology [9,10].

In this work, nine nanogel formulations containing 1% w/w *T. grandis* seed extract nanoparticles were prepared and evaluated. These formulations were assessed for critical properties, including flowability, pH, spreadability and drug permeation. The findings revealed that nanogels effectively maintain higher drug concentrations across the skin barrier for extended periods, particularly for the hydrophobic drugs [11-13].

EXPERIMENTAL

Tectona grandis seeds extract was obtained from seeds collected from the Banaras Hindu University (BHU) campus, Varanasi, India. The external shells of the seeds were carefully removed before washing. After washing, the seeds were air-dried to ensure complete removal of moisture. Once fully dried, the seeds were finely ground and stored in a moisture-free, sealed container for future use. The other ingredients were of analytical grade also prepared accordingly. The required vehicles were prepared using twice-distilled water and protected from light to prevent any photochemical reactions during the research process.

Preparation of *Tectona grandis* seed extract: Powdered *Tectona grandis* seeds (5 g) were weighed, mixed with 50 mL distilled water and then heated in water bath at 80 °C for 15-20 min. Afterward, the extract was filtered to eliminate unwanted particles. The capacity was adjusted to 100 mL with distilled water and the product was stored at 4 °C [14,15].

Synthesis of silver nanoparticles: The AgNO₃ solution (1 mM) as well as *T. grandis* seed extract were added together in a 1:9 proportion. The reaction solution was maintained just below its boiling point and continuously stirred at 800 rpm using a magnetic stirrer. Within 1 h, the solution changes to a reddish-brown in colour, indicating the formation of silver nanoparticles. This entire synthesis process was conducted in absence of light to prevent any photochemical reactions.

The resulting suspension was then centrifuged at 15,000 rpm for 45 min and washed 3-4 times using deionized water to eliminate any residual silver ions and seed extract. The nano-

particles were kept in a cool, dry and dark environment for further analysis [16].

Characterization: The UV-visible spectrum of synthesized AgNPs was evaluated with a UV-1800 Shimadzu spectrophotometer in the wavelength range of 300-600 nm. The FT-IR analysis of nanoparticles was studied with a Spectrum 8900 IR Spectrometer (Shimadzu, Tokyo, Japan) to detect key functional groups inside the seed extract and also its involvement during the production and stabilization of silver nanoparticles. The measurement was conducted in transmittance mode and wavenumber range of 4000 to 400 cm⁻¹. Particle size was determined using a nano particle size analyzer (Malvern Zeta Sizer). To ensure accurate measurements, the sample concentration was kept below 1 g/L and diluted at a 1:100 ratio. The prepared sample was then loaded into the analyzer cell and the Zetasizer software was activated to measure the particle size distribution. For zeta potential analysis, the sample was transferred into a clear polystyrene cuvette with a path length of 1 cm also positioned in a thermostatic sample chamber kept at 25 °C and finally measured with the MALVERN software. FESEM and EDX analysis were conducted with a Quanta 200F Netherlands, instrument equipped with an xT microscope (Olympus, CH20) control and a tungsten filament as the source. TEM analysis was carried out with a TECTNA 12 200F, Netherlands, utilizing TECNAI imaging and analysis software, with a tungsten filament as the electron source.

Formulation of nanogel: The nanogel loaded with extract of *T. grandis* seed was prepared using dispersion method, following the concentrations as specified in Table-1. Carbopol 934 was initially dispersed in distilled water and left to swell for 2 h before further processing. After swelling, the mixture was stirred using a magnetic stirrer and the required amount of *T. grandis* seed extract-loaded nanoparticles was incorporated to achieve a 1% concentration in gel. Accurately weighed silver nanoparticle, Eudragit S-100 (polymer) and Tween-80 as stabilizer are dissolved in glycerol while stirring. Prepared aqueous phase containing Carbopol-940 dissolved in water with continuous stirring and heat. These drugs containing phase is sonicated on ultrasonic bath sonicator. The drug phase is added drop by drop into the aqueous phase during homogenization to form emulsion. The emulsion converted into nanodroplets by homogenizer which formed O/W emulsion. Homogenization was continued for 1 h, resulting in a smooth and uniform gel. The homogenization process continued until Carbopol 934

TABLE-1
FORMULA FOR DIFFERENT FORMULATIONS

Batches	Ag NPs (g)	Carbopol (g)	Eudragit S (g)	Tween 80 (mL)	Glycerol (mL)
F1	0.1	0.5	0.15	0.5	5
F2	0.5	0.1	0.15	0.5	5
F3	0.1	0.1	0.15	0.5	5
F4	0.5	0.5	0.15	0.5	5
F5	0.1	0.1	0.25	0.5	5
F6	0.5	0.1	0.25	0.5	5
F7	0.1	0.5	0.02	0.5	5
F8	0.3	0.5	0.02	0.5	5
F9	0.3	0.3	0.02	0.5	5

was fully dispersed, resulting in a smooth and uniform gel. Finally, triethanolamine was added to adjust the pH of the formulation to a range of 6.1-6.8, ensuring the gel had an optimal consistency and appearance [13,17,18]. The prepared nanogel was subsequently evaluated for pH, viscosity, spreadability, washability and antibacterial activity.

Evaluation parameters of nanogels

Physical evaluation: The nanogels were thoroughly evaluated for various physical characteristics including colour, odour, homogeneity and texture. The colour and odour of the nanogel were visually assessed to ensure consistency and suitability for topical applications. Homogeneity was checked by examining the uniform distribution of components throughout the gel, while the texture was evaluated to ensure smoothness and absence of any irregularities. These evaluations are critical for confirming the quality and potential acceptability of the nanogel for pharmaceutical use.

pH: The nanogel pH was determined with a calibrated pH meter (Polmon, LP-139S) by immersing the electrode in the sample after calibration with standard buffer solutions. The reading was taken after stabilization and repeated in triplicate for accuracy. If needed, the pH was adjusted within the desired range (6.0-7.5) and the electrode was rinsed with distilled water after each measurement.

Spreadability: The spreadability of the nanogel was evaluated using a simple method involving a glass plate. A fixed amount of nanogel (1-2 g) was placed upon clean glass plate. Another glass plate, weighed (100 g), was positioned upon top of the sample. The distance the gel spread under the weight was measured after a specified period (*e.g.* 1 min). The spreadability was determined by observing the uniformity of the spread and calculating the spread area. The spreadability of the nanogel reflects its ease of application on the skin, which is critical for its effectiveness in topical use.

Washability: A small amount of nanogel was applied to the skin and left for 30 min. The area was then rinsed with lukewarm water and the ease of removal was assessed based on the time taken to wash off and any remaining residue. The washability was classified as easy, moderate or difficult, which assessed the suitability of gel for practical topical application.

Viscosity: Brookfield DV-E Viscometer was used to determine the viscosity. The samples were tested at various speeds (10, 20, 50, 60 and 100 rpm) using spindle number 64. The viscosity readings were recorded at each specified speed to assess the flow properties of the nanogels.

Antibacterial activity: Antibacterial activity of the nanogel was evaluated using the agar well diffusion method [19]. *Escherichia coli* was cultured overnight in sterile nutrient broth. Agar plates inoculated with the bacterial strains were prepared and wells were made in the agar. The formulated gel was then placed into the wells and then the plates were incubated at 37 °C for 24 h. The zones of inhibition surrounding the wells were calculated to assess the antibacterial effectiveness of the nanogel.

Wound healing activity: This activity was evaluated using an incision wound model on rats. Animal experiments were

performed with prior approval (CPCA number 1858) of animal ethical committee of Sandip Institute of Pharmaceutical Science, Nashik, India. After creating a standardized wound under aseptic conditions, rats were separated into two sets *viz.* (i) control group (placebo gel) and (ii) the test group (treated with the prepared nanogel). The nanogel was applied topically once daily for 14 days. Wound healing was monitored by measuring the wound area at regular intervals (days 0, 7 and 14) to assess the rate of contraction. Wound contraction percentage was calculated to determine the extent of healing. Moreover, the visual observations of wound closure, formation of new connective tissue, also skin regeneration were observed to evaluate the progression of healing [20].

RESULTS AND DISCUSSION

Visual observation: A colour change from yellowish-brown to dark brown was observed following the addition of AgNO₃ to the seed extract indicating the biosynthesis of silver nanoparticles.

UV-visible spectral studies: The absorbance spectrum of synthesized silver nanoparticles (AgNPs), shown in Fig. 1, exhibit a distinct peak at 440 nm, corresponding to surface plasmon resonance (SPR). This peak arises from the collective oscillation of surface electrons upon light interaction, indicating the successful formation and stability of AgNPs.

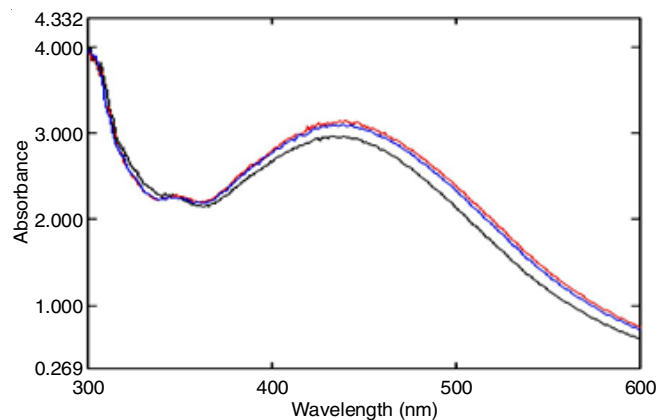


Fig. 1. Absorbance spectra of silver nanoparticles obtained at different time intervals

FTIR spectral studies: The FTIR spectrum of *Tectona grandis* seed extract based AgNPs is shown in Fig. 2. The IR peaks indicate the presence of various compounds like proteins, carboxylic acids and amines, contribute to the reduction and stabilization of silver nanoparticles during synthesis. The FTIR spectrum revealed bands at 1745, 1643, 1508 and 1038 cm⁻¹, which correspond to the stretching vibrations of the C=O bond of carboxylic acids or esters, the N-C=O amide bond of proteins, nitro compounds and the C-N amine bond, respectively. The other details of the peaks in the synthesized AgNPs are presented in Table-2, suggesting that the functional groups in the seed extract play a role in the formation and stabilization of AgNPs.

Particle size analysis: The results shown in Fig. 3 indicated that the particle size of the synthesized AgNPs is approximately 140 nm. The particle size of up to 80-90 nm show a

TABLE-2
FTIR SPECTRAL DATA AND FUNCTIONAL GROUP OF SILVER NANOPARTICLES

Functional group	Wavenumber (cm ⁻¹)	Role
O-H stretching	3600-3400	Indicates tannins and phenolic compounds; antioxidant properties.
C=O stretching	1650-1630	Suggests flavonoids; enhances wound healing.
N-H stretching	3300-3200	Indicates alkaloids; provides analgesic effects.
C-O stretching	1350-1280	Indicates phenolic compounds; supports tissue repair.
C-H stretching	3000-2800	Indicates fatty acids; promotes skin hydration.
C-O stretching (glycosides)	1200-1000	Indicates saponins; enhances antimicrobial activity.

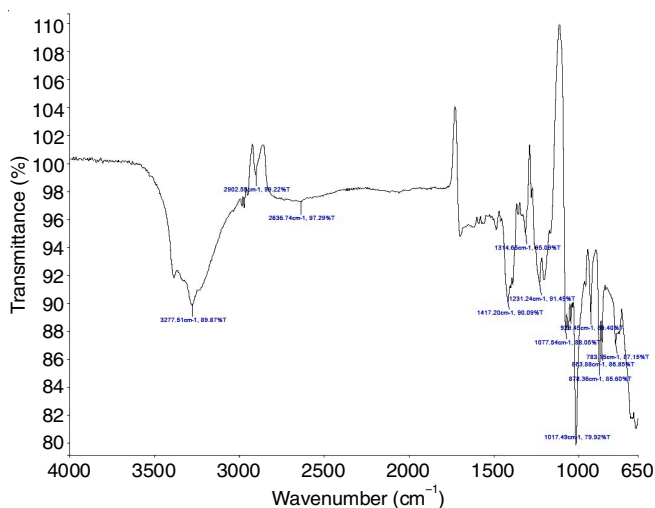


Fig. 2. FTIR spectra of silver nanoparticles

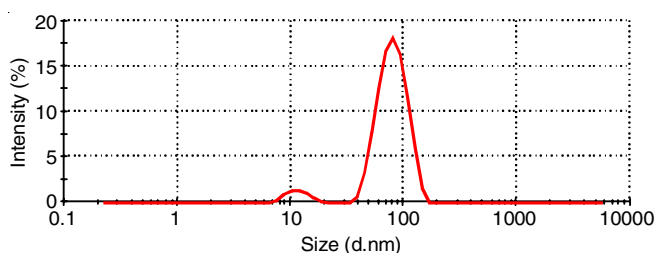


Fig. 3. Particle size of lyophilized powder

crucial part in improving the tissue diffusion and bioavailability of nanoparticles. Nanoparticles within this size range are small enough to effectively permeate through the skin's layers, allowing for better delivery of active ingredients to the target site. This size also enhances the solubility and stability of the encapsulated compounds, ensuring the sustained release over time. Furthermore, nanoparticles with sizes around 140 nm have been shown to possess antimicrobial properties, making them highly effective in inhibiting bacterial growth [21]. These attributes—enhanced tissue penetration, improved bioavailability and antimicrobial effects—make nanoparticles ideal candidates for developing wound healing formulations.

Zeta potential: The zeta potential of -12.8 mV for AgNPs synthesized from *T. grandis* seed extract offers significant insight into their stability and potential effectiveness in wound healing applications. This negative zeta potential value indicates that the AgNPs carry a moderate negative charge. The negative charge facilitates the electrostatic repulsion between similarly charged particles, which helps prevent aggregation and contributes to the stability of the nanoparticles (Fig. 4).

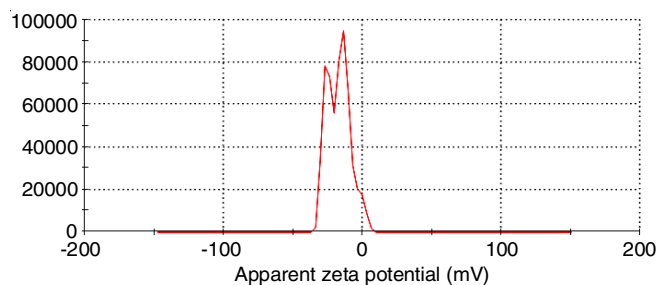


Fig. 4. Zeta potential of lyophilized powder

Morphological studies: FESEM analysis clearly reveals the occurrence of synthesized AgNPs, which exhibit oval and circular shapes. While utmost nanoparticles tend to aggregate, a few are observed as individual particles, indicating some degree of dispersion (Fig. 5a). The spherical and oval shapes of the nanoparticles are advantageous for wound healing applications, as these forms can improve interactions with biological tissues. The observed aggregation of most nanoparticles may enhance their efficacy by increasing the surface area available for interaction with wound exudates, thereby facilitating the release of therapeutic agents. Fig. 5b clearly demonstrates that the synthesized nanoparticles possess suitable morphology and contain silver, validating their potential as effective candidates for wound healing formulations.

Transmission electron microscopy (TEM): The TEM image (Fig. 6) exposed the synthesized AgNPs predominantly fall inside the size range of 10 to 70 nm. This small particle size is highly beneficial for biomedical applications, as it improves the nanoparticles' ability to penetrate biological tissues, which can accelerate the healing process [22]. Moreover, the increased surface area-to-volume ratio of smaller nanoparticles enhances their interactions by microbial cells, making them more effective in disrupting bacterial membranes and inhibiting bacterial growth.

Evaluation parameters of nanogels

All formulations displayed a clear, consistent colour and odourless. The visual inspections confirmed that all formulations were homogeneous, free from grittiness or particulate matter, indicating that the nanogels were well-prepared and stable.

pH: The pH values of the nanogel batches were measured (Table-3), revealing slight variations among the different formulations. The pH values ranged from 7.63 to 8.03. Specifically, batches F1, F4, F6 and F7 all exhibited a pH of 7.73, while batches F2 and F3 showed slightly lower values of 7.63. Batch F5 had the highest pH at 8.02 and batch F8 showed a similar

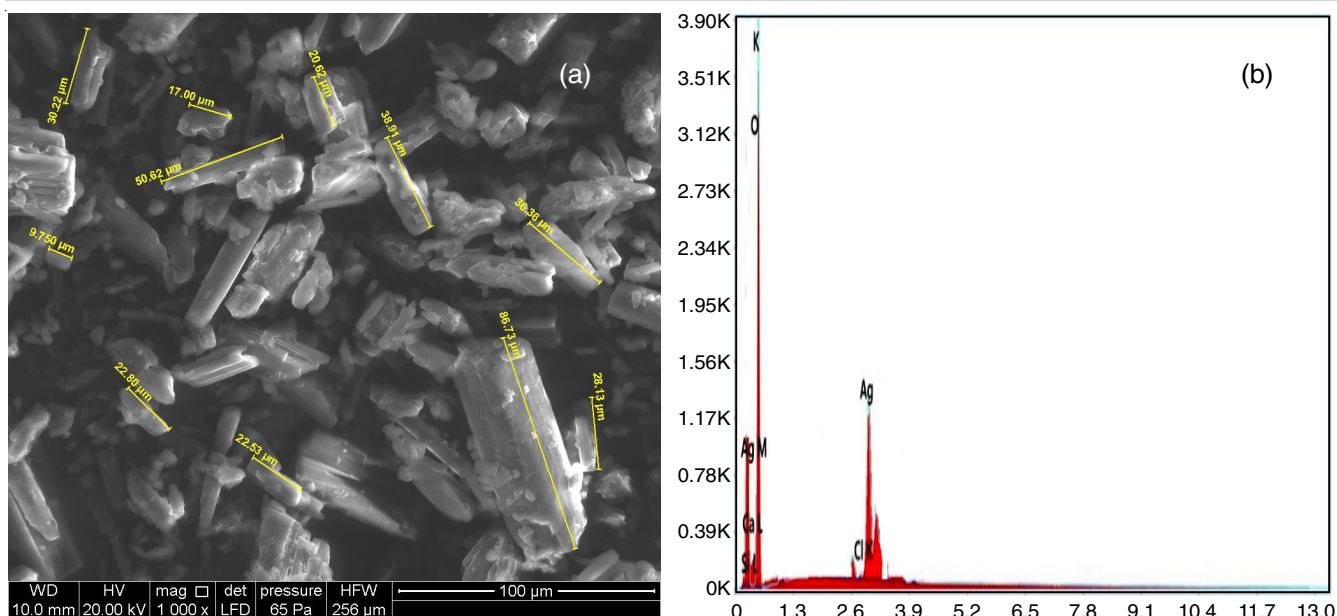


Fig. 5. FESEM-EDX image of synthesized silver nanoparticles

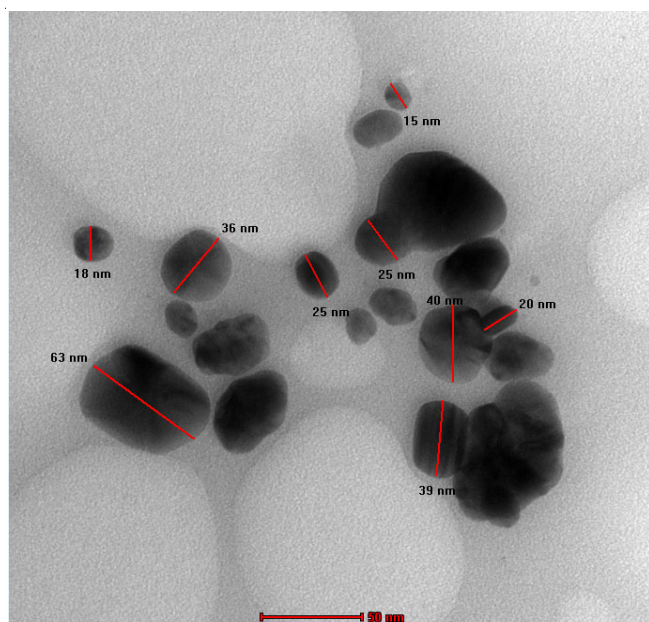


Fig. 6. TEM image of AgNPs

TABLE-3
pH VALUES OF ALL BATCHES AND
SPREADABILITY (g cm/s) OF NANOGELS

Batch number	pH value	Spreadability (g cm/s)
F1	7.73	9.6
F2	7.63	10.3
F3	7.63	9.6
F4	7.73	9.6
F5	8.02	10.6
F6	7.73	10.7
F7	7.73	9.6
F8	8.03	10.9

pH value of 8.03. The pH levels observed are nearly neutral, making them suitable for applications on the skin, as they are less likely to induce irritation or interfere with the skin's natural

protective layer. The minor variations in pH may be due to the different formulation compositions but still fall within a suitable range for effective topical use.

Spreadability: The spreadability of the nanogels ranged from 9.6 g cm/s to 10.9 g cm/s, indicating moderate spreadability (Table-3). This range suggests that the nanogels are well-suited for effective application on the skin, providing ease of spreading while maintaining stability and ensuring controlled drug release characteristics.

Washability: Positive feedback was received regarding the ease of removal and comfort during washing. These results suggest that the nanogels possess good washability, making them user-friendly for practical applications.

Viscosity: It was evaluated at different rotational speeds, as shown in Table-4. At lower speeds (10 and 20 rpm), the viscosity was higher, with values of 3340 cP and 1854 cP, respectively. These higher viscosity values were expected, indicating a thicker consistency at lower shear rates. As the speed increased to 50, 60 and 100 rpm, the viscosity decreased significantly, with values of 927 cP, 794 cP and 573 cP, respectively. This reduction in viscosity at higher speeds suggests that the nanogels exhibit shear-thinning behaviour, where their viscosity decreases under higher shear forces, a desirable property for easy application and spreadability.

TABLE-4
VISCOSITY OF NANOGELS AT DIFFERENT rpm

Speed (rpm)	Viscosity (cP)	Notes
10	3340	Higher viscosity expected
20	1854	Higher viscosity expected
50	927	Lower viscosity expected
60	794	Lower viscosity expected
100	573	Lower viscosity expected

Batch F1 emerges as the most balanced and effective formulation based on above evaluation. It displayed a neutral pH of 7.73, which is ideal for skin applications, ensuring mini-

mal irritation. Its moderate spreadability of 9.6 g cm/s ensures ease of application while maintaining stability. Additionally, Batch F1 exhibited desirable shear-thinning behaviour with high viscosity at lower speeds (3340 cP at 10 rpm) and significant reduction at higher speeds (573 cP at 100 rpm), enabling smooth application and effective spreadability. Along with clear appearance, homogeneity and good washability, these properties collectively highlight Batch F1 as the most stable, user-friendly and well-prepared formulation and hence selected for further studies.

Antibacterial activity: Fig. 7 displays the results of the antibacterial activity test for the nanogel in contradiction of *E. coli* by means of agar diffusion technique. The two wells, labeled 5 mg and 100 mg, demonstrate the antibacterial efficacy of the nanogel (F1) at different concentrations. Nanogel showed the largest zone of inhibition (50 mm), indicating strong antibacterial activity. The larger zone of inhibition observed in the well with 100 mg suggests that the nanogel exhibits dose-dependent antibacterial activity, with the 100 mg concentration showing a stronger effect. In terms of wound healing, the strong antibacterial activity of the nanogel is beneficial for preventing infections in wound sites. By inhibiting bacterial growth, it can reduce the risk of infection and promote faster healing. The

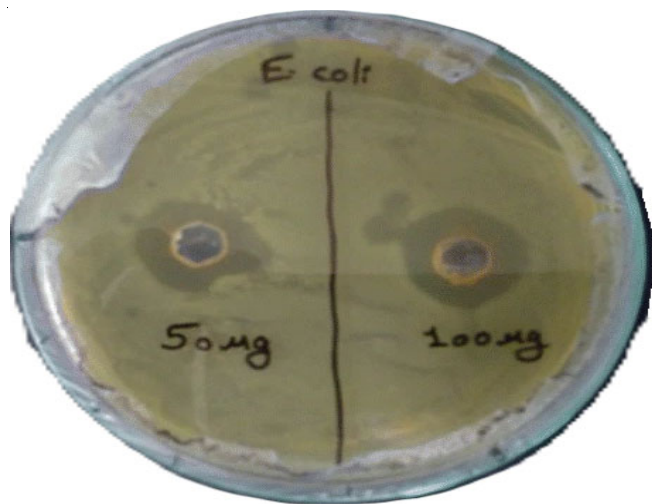


Fig. 7. Antibacterial activity for nanogel

presence of a significant zone of inhibition (50 mm) confirms that the nanogel could play a critical role in treating infected wounds, making it a promising candidate for wound care formulations [23,24].

Wound healing activity: The results disclosed important improvement in the wound healing process in the test group treated with *T. grandis* seed extract nanogel (F1) compared to the control group. On day 7, the treated group exhibited remarkable wound contraction with the formation of granulation tissue, indicating the initiation of healing. By day 14, the wound in the treated group had almost completely closed, with visible re-epithelialization and minimal scar formation (Fig. 8). In contrast, the control group displayed slower wound contraction and delayed healing progression by day 14 (Fig. 9). These findings suggest that the nanogel effectively accelerates the wound healing process, likely due to the anti-inflammatory and regenerative properties of *T. grandis* seed extract.

The nanogel formulations exhibited promising results for wound healing applications. The pH values (7.63 to 8.03) were close to neutral, making them suitable for skin application with minimal irritation. Spreadability ranged from 9.6 g cm/s to 10.9 g cm/s, ensuring easy application while maintaining stability. The nanogels also showed excellent washability, making them user-friendly. Viscosity decreased with increasing rpm, indicating shear-thinning behaviour, which is ideal for both smooth application and stability. The nanogels demonstrated strong antibacterial activity, with a 50 mm ZOI against *E. coli*, highlighting their potential for preventing infections in wounds. The incorporation of *T. grandis* seed extract further amplified wound healing activity due to its well-documented anti-inflammatory, antioxidant and collagen-stimulating effects. These extracts promote granulation tissue formation, enhance hydroxyproline levels and accelerate epithelial tissue repair [25]. Thus, the physical characteristics and antibacterial activity of nanogels render them fascinating possibilities for wound healing formulations.

Conclusion

Tectona grandis seed extract was used as a reducing and stabilizing agent in the study, which effectively demonstrated a green synthesis of silver nanoparticles. The crystalline struc-



Fig. 8. Wound healing progress in treatment group; (a) fresh incision wound (day 0), (b) partial wound healing (day 7) and (c) significant wound closure (day 14)

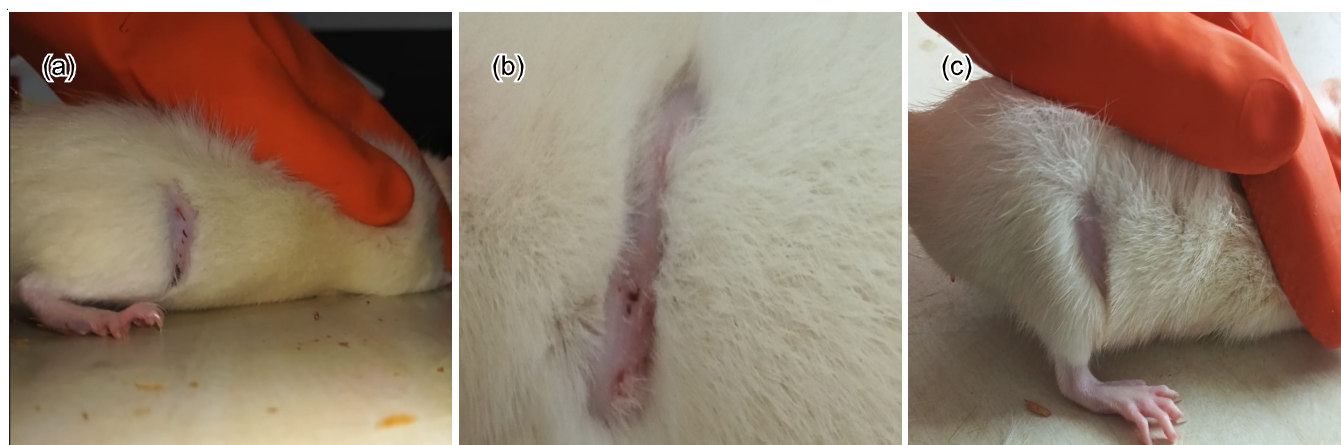


Fig. 9. Wound healing progress in controlled group; (a) fresh incision wound (day 0), (b) partial wound healing (day 7) and (c) significant wound closure (day 14)

ture and stability of the synthesized AgNPs were validated by X-ray diffraction, UV-visible spectroscopy and transmission electron microscopy, which revealed that their diameters ranged from 32 to 62 nm. The antibacterial activity of the synthesized AgNPs was significant, with strong inhibition observed against *E. coli*, exhibiting their potential as antimicrobial agents. Moreover, the nanogels formulated with these AgNPs displayed optimal pH, spreadability, viscosity and washability, making them suitable for topical applications. The nanogels display remarkable wound healing potential, as evidenced by the excision wound model. A progressive reduction in wound size was observed over the evaluation period, with batch F1 exhibiting the most accelerated healing. Significantly, complete wound closure was achieved within 14 days, significantly outperformed the control group, which displayed a slower recovery trajectory. This accelerated healing can be attributed to the synergistic action of the antibacterial properties of AgNPs and the therapeutic components of *T. grandis* seed extract, which promote tissue regeneration and infection control. Overall, this study contributes valuable insights into sustainable practices in nanomaterial development while addressing growing health concerns related to antibiotic resistance and wound management.

ACKNOWLEDGEMENTS

The authors sincerely thank the School of Pharmaceutical Sciences, Sandip University, Nashik, India for the resources and support provided for this research.

CONFLICT OF INTEREST

The authors declare that there is no conflict of interests regarding the publication of this article.

REFERENCES

- M. Arif, A. Rauf and T. Akhter, *RSC Adv.*, **14**, 19381 (2024); <https://doi.org/10.1039/D4RA02467B>
- S.D. Ghaywat, P.S. Mate, Y.M. Parsutkar, A.D. Chandimeshran and M.J. Umekar, *GSC Biol. Pharm. Sci.*, **16**, 40 (2021); <https://doi.org/10.30574/gscbps.2021.16.1.0196>
- N. Raina, R. Rani, V.K. Thakur and M. Gupta, *ACS Omega*, **8**, 19145 (2023); <https://doi.org/10.1021/acsomega.2c08016>
- X. Zhang, S. Yan, R.D. Tyagi and R.Y. Surampalli, *Chemosphere*, **82**, 489 (2011); <https://doi.org/10.1016/j.chemosphere.2010.10.023>
- A.V. Kabanov and S.V. Vinogradov, *Nanogels as Pharmaceutical Carriers, Multifunctional Pharmaceutical Nanocarriers*, Springer Science: New York, pp. 67-80 (2008).
- C. Suryakumari, M. Narender, K. Umasankar, S.P. Panda, S.N.K. Rao and S. Panda, *J. Drug Deliv. Ther.*, **9**, 110 (2019); <https://doi.org/10.22270/jddt.v9i6-s.3770>
- S. Gupta, J. Gupta, A. Anand and S. Ojha, *Biol. Sci.*, **2**, 269 (2022); <https://doi.org/10.55006/biolsciences.2022.2304>
- S.M.B. Asdaq, N. Nayeem, Abida, M.T. Alam, S.I. Alaqel, M. Imran, E.-W.E. Hassan and S.I. Rabbani, *Saudi J. Biol. Sci.*, **29**, 1456 (2021); <https://doi.org/10.1016/j.sjbs.2021.11.026>
- K. Manimaran, *Biomass Convers. Biorefin.*, **14**, 15011 (2024); <https://doi.org/10.1007/s13399-023-04072-5>
- V. Rajput, T. Minkina, M. Mazarji, S. Shende, S. Sushkova, S. Mandzhieva, M. Burachevskaya, V. Chaplygin, A. Singh and H. Jatav, *Ann. Agric. Sci.*, **65**, 137 (2020); <https://doi.org/10.1016/j.aosas.2020.08.001>
- J.S. Kim, S.D. Jo, G.L. Seah, I. Kim and Y.S. Nam, *J. Ind. Eng. Chem.*, **21**, 1137 (2015); <https://doi.org/10.1016/j.jiec.2014.05.026>
- H. Rosaini, A. Halim, I.E. Sandi, I. Makmur, R. Asra and W.M. Sidoretno, *Int. Res. J. Pharm.*, **12**, 21 (2021); <https://doi.org/10.7897/2230-8407.1201112>
- X. Li, W. Li, M. Wang and Z. Liao, *J. Control. Release*, **335**, 437 (2021); <https://doi.org/10.1016/j.jconrel.2021.05.042>
- J. Annamalai and T. Nallamuthu, *Appl. Nanosci.*, **6**, 259 (2016); <https://doi.org/10.1007/s13204-015-0426-6>
- Z. Gün Gök, A. Demiral, O. Bozkaya and M. Yigitoglu, *Polym. Bull.*, **78**, 7241 (2021); <https://doi.org/10.1007/s00289-020-03486-9>
- A.M. Alwan, R.A. Khamis and S.M. Abdallah, *Iraqi J. Sci.*, **26**, 1274 (2019); <https://doi.org/10.24996/ijis.2019.60.6.11>
- Y.S. Sujitha and Y.I. Muzib, *Int. J. Pharm. Investig.*, **10**, (2020); <https://doi.org/10.5530/ijpi.2020.4.87>
- P. Yadav, S. Pandey and S.K. Dubey, in eds.: K.A. Abd-El Salam, A.F. Hashim, F.K. Ahmed and S. Thomas, *Nano-Enhanced Biopolymers for Antimicrobial Applications*, In: *Biopolymeric Nanoparticles for Agricultural Applications*, Springer, Cham, pp. 175-208 (2024).
- Y. Fan, M. Lüchow, Y. Zhang, J. Lin, L. Fortuin, S. Mohanty, A. Brauner and M. Malkoch, *Adv. Funct. Mater.*, **31**, 2006453 (2021); <https://doi.org/10.1002/adfm.202006453>
- Y.P. Talekar, K.G. Apte, S.V. Paygude, P.R. Tondare and P.B. Parab, *J. Ayurveda Integr. Med.*, **8**, 73 (2017); <https://doi.org/10.1016/j.jaim.2016.11.007>
- J.A. Garza-Cervantes, G. Mendiola-Garza, E.M. de Melo, T.I.J. Dugmore, A.S. Matharu and J.R. Morones-Ramirez, *Sci. Rep.*, **10**, 7281 (2020); <https://doi.org/10.1038/s41598-020-64127-9>
- N. Hoshyar, S. Gray, H. Han and G. Bao, *Nanomedicine*, **11**, 673 (2016); <https://doi.org/10.2217/nmm.16.5>
- R. Yahya and N.M. Alharbi, *Int. J. Biol. Macromol.*, **253**, 127080 (2023); <https://doi.org/10.1016/j.ijbiomac.2023.127080>
- A. Sharma, C. Verma, S. Mukhopadhyay, A. Gupta and B. Gupta, *ACS Appl. Nano Mater.*, **5**, 8546 (2022); <https://doi.org/10.1021/acsnanm.2c01959>
- R. Shivhare and N. Jain, *J. ReAttach Therapy Develop. Div.*, **6**, 1825 (2023); <https://doi.org/10.53555/jrtdd.v6i9s.2489>